2024 IEEE/RSJ International Conference on Intelligent Robots and Systems (IROS)
October 14-18, 2024. Abu Dhabi, UAE

Discover2Walk: A cable-driven robotic platform to promote gait in pediatric population

Pablo Romero-Sorozabal, Gabriel Delgado-Oleas, Annemarie F Laudanski *Member IEEE*, Álvaro Gutiérrez *Senior Member IEEE* Eduardo Rocon , *Member IEEE*

***Abstract*— Recent advancements in gait rehabilitation have led to the development of innovative approaches that complement traditional therapeutic methods. These include intense, task-specific exercise strategies, non-invasive treatments, surgical interventions, and advanced robotic technologies. While robotic systems for adult gait rehabilitation are well-established, there is a notable scarcity of such devices for pediatric patients, especially toddlers, due to their unique developmental and biomechanical needs. This work introduces Discover2Walk (D2W), a novel robotic platform designed specifically for pediatric gait rehabilitation in small children. The D2W platform features a multi-module, cable-driven architecture guided by an omnidirectional traction module, addressing the limitations of current rehabilitation devices for younger populations. The platform's modular design consists of three actuated modules—pelvic, ankle, and traction—synchronized by a personalised gait pattern generator. This configuration allows for simultaneous control and monitoring of pelvic and ankle motion using partial body weight support and Assistance As Needed (AAN) approaches. Preliminary evaluations were conducted with pediatric patients with Cerebral Palsy, involving two ambulatory six-year-olds and one non-ambulatory four-year-old, over a series of 10 gait rehabilitation sessions. Data analysis from the ambulatory children showed a decrease in the robotic effort required to assist limb movements along healthy trajectories throughout the sessions, accompanied by an increase in walking speeds. Further work will include expanding the patient cohort to include a broader range of ages, sizes and GMFCS levels to validate the system's effectiveness across a wider spectrum of pediatric gait disabilities and validating the traction effectiveness.**

I. Introduction

Over the last few decades, there has been growing interest in the development of robotic platforms designed for assistance/rehabilitation. The benefits of these devices stem from their ability to deliver controlled training assistance during therapies and to generate precise quantitative data of the patient's performance, [1]. Numerous systems have emerged specifically for gait training rehabilitation, including well-known examples such as: Lokomat [2], LOPES [3], and CPWalker (by our research group) [4], to name but a few. Although there is a considerable number of these robots for rehabilitation of adults, they are still scarce for children [5], due to the peculiarities of this population, [6], [7]. Researchers have created mobile robots to improve crouch gait, [8], that the infant can ride, [9], to promote crawling, [10], or body weight support systems to promote motor learning [11]. These approaches, while potentially giving the child some sense of independent mobility, do not encourage developing any motor skills (limited benefits) or very constrained training. Early active movement is essential because toddlers with CP who do not attempt to walk may lose their limited number of corticospinal connections, which seems a major cause of disability, [12].

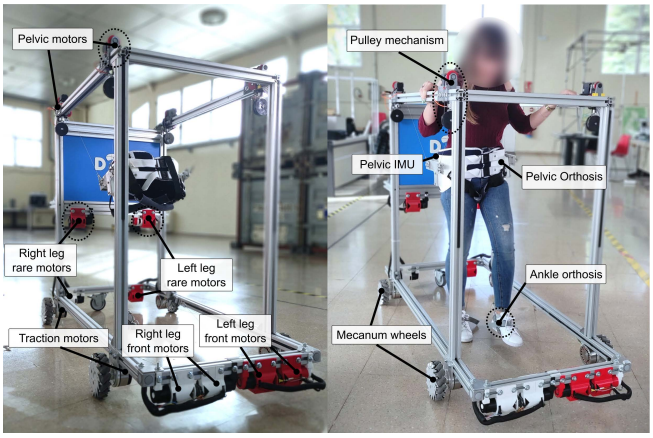

Fig. 1. Overview of the full Discover2Walk (D2W) platform. Left image: picture of the D2W platform and actuators positions. Right image: system components of the system highlighted while the platform is used by a healthy subject.

This article introduces the Discover2Walk (D2W), a pediatric gait rehabilitation platform that employs a multi-module structure based on cable-driven robotics to aid in gait assistance during the initial motor development stages of children with Cerebral Palsy (CP). The study offers a thorough examination of the system's design, encompassing its architecture, mechanical aspects, and electronics. Additionally, it delves into the intricacies of the control

*This research was funded by the Spanish Ministry of Science and Innovation, project Discover2Walk (PID2019-105110RB-C31). PRZ received a Training Program fellowship (PRE2020-092049) from the Ministry of Science and Innovation.

Pablo Romero-Sorozabal , Gabriel Delgado-Oleas and Eduardo Rocon are with the Centro de Automática y Robótica, Consejo Superior de Investigaciones Científicas–Universidad Politécnica de Madrid (CSIC-UPM), 28040 Madrid, Spain. (e-mail: p.romero@csic.es).

Gabriel Delgado-Oleas is also with Universidad del Azuay, Cuenca, Ecuador.

Annemarie F Laudanski is with Dalhousie University, Nova Scotia, Canada.

Álvaro Gutierrez is with ETSI Telecomunicación, Universidad Politécnica de Madrid, Madrid, España.

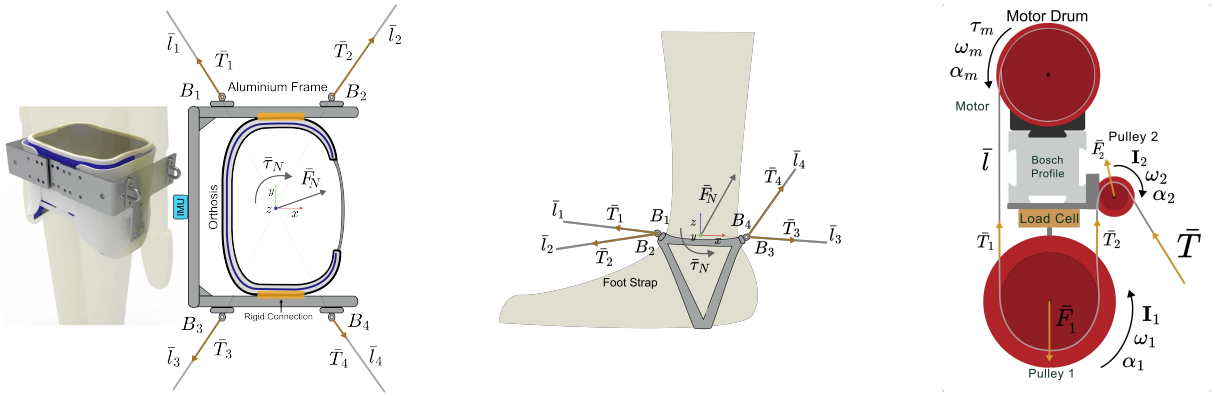

a) Pelvis orthosis. *b) Ankles orthosis* *c) Pelvis pulley mechanism.*

Fig. 2. Discover2Walk orthosis and pulley mechanisms.

strategies employed by D2W. Preliminary validation results for the D2W are also presented, providing valuable insights into its efficacy and potential impact.

II. Design of the Discover2Walk

A. Robotic Platform Design

Existing assistive robots are inappropriate for toddlers due to their rigid structure and traditional actuators, which limit the child's ability to guide the therapy and explore their own motor repertoire, [13]. Thus, such rigid and cumbersome form factor of current technology are incompatible with the dynamic movements and pliable limbs of toddlers, which often lead to increase the risk for lesions due to excessive pressure to the skin. The following sections detail the design rationale behind the development of the Discover2Walk system, which is engineered to facilitate toddler support during upright gait, aid in breathing, and provide assistance with weight-bearing, [14].

1) Discover2Walk structure

Traditionally, robotic platforms consist of rigid links and mechanical joints placed alongside the human limbs to enhance/assist patient joints motion, [15]. Despite their promising results across a range of neuro-pathologies, there is an increasing shift towards exploring the potential benefits of integrating flexible actuators over traditional rigid ones, [16].

The design of Discover2Walk is founded upon a cable-driven solution, which effectively tackles various challenges associated with rigid designs, such as the inertia of added weight and potential misalignments in human-robot joints [17], [18]. Several cable-driven devices have already demonstrated their efficacy in gait rehabilitation applications, such as THE FLOAT for body weight support during gait [19], A-TPAD for studying force adaptations at the pelvis during human walking [20], and CDLT, a gait training machine comprising a body weight support system and a cable-driven parallel orthosis, [21]. Drawing inspiration from these solutions, Discover2Walk features a structure crafted from aluminum profiles (BOSCH, Germany), forming a rectangular prism (0.89x0.65x1.2m), which accommodates the pelvic, ankle, and traction modules (Fig. 1). The subsequent paragraphs elaborate on the specific solutions implemented for each component of the Discover2Walk system.

a) Pelvic Module

The pelvic module consists of a suspended parallel system driven by four cables designed for partially body-weight support and control of pelvic position and orientation. The patient's pelvis is securely connected to the system by attaching the module's cables to a modified commercial hip orthosis (PRIM, Spain). This modification consists of a "U" shaped rigid aluminium frame attached to the lateral sides of the orthosis, allowing the cables tensions to be transmitted to the pelvis while reducing potential energy losses resulting from the orthosis' flexible materials (Fig. 2a).

Nylon coated 7x19 316 Marine Grade Stainless Steel cables (TECNI, United Kingdom) with a maximum breaking load (MBL) of 22kg are used in this module. These cables were selected due to their small diameter, flexibility, and tensile strength capable of controlling motion and supporting bodyweight in children up to 30kg.

Actuation. To control the patient's pelvis position and bodyweight support the pelvic module uses four Dynamixel XH540-W150-T servomotors (ROBOTIS, United States) symmetrically arranged at the platform's top corners (Fig. 1). These control the pelvic' cable lengths and allow ≤7.1Nm (stall torque) and 70rpm no load velocity which translates to: ≤51.7Kg per cable and cable speeds of 0.102m/s for drum radii of 0.014m.

Sensors. To monitor the pelvis motion and control the partial bodyweight support, the pelvic module includes three main types of sensors: inertial measurement units (IMUs), motor absolute encoders, and load cells. A BNO055 IMU sensor (BoschSensortec, Germany), composed of a triaxial accelerometer, gyroscope and geomagnetic with I2C, UART available communication protocols, was attached to the pelvic orthosis. The IMU placed in the back of the pelvic orthosis is used to monitor the pelvis orientation (rotation, tilt and obliquity), velocities and accelerations. Data from the motors' embedded absolute encoders, used to measure cable lengths, are combined with the IMU-based pelvis orientation to compute the pelvis position with respect the frame origin of coordinates through forward kinematics through the numerical methods explained below, [22].

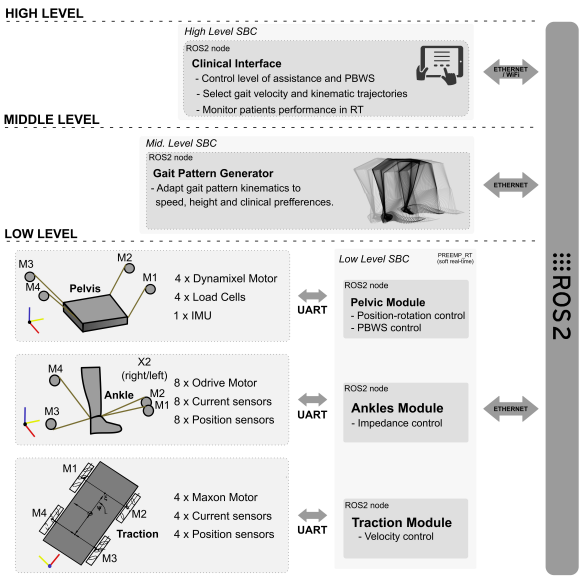

Fig. 3. General architecture of the Discover2Walk system. The system is divided into three hierarchical levels. At the high level, a clinical interface allows configuration and monitoring of the robotic therapy prescribed; at the middle level, the gait pattern generator synchronizes the low-level modules; and at the low level, the pelvic, ankles, and traction modules sense and control the joint motions following the setpoints of the gait pattern generator. All programs are built as ROS2 nodes running on single board computers (SBCs) (one per level) which communicate via Ethernet/WiFi.

The weight supported by each cable of the pelvic module is measured using a DYMH-103 load cell with a maximum capacity of 20Kg (CALT sensor, China), placed inside a custom pulley mechanism for each motor. This system of pulleys allows the cable real tension (T) to be calculated from the measured reaction force F, where $F = f(T)$, (Fig. 2c). The design mechanism's dynamics are described as:

$$F_1 = T_1 - T_2 - m_1 \cdot a_1 \quad (1)$$

$$T_1 = \frac{I_1 \cdot \alpha_1}{r_1} + T_2 \quad (2)$$

$$T = \frac{I_2 \cdot \alpha_2}{r_2} + T_1 \quad (3)$$

Assuming that the pulleys and load cell are static and that the cable and pulley masses are negligible when compared to the end-effector mass, then, from (2) and (3), $T \approx T_1 \approx T_2$, where T_1 and T_2 are the cables tensions form the motor drum to pulley 1 and form pulley 1 to pulley 2, therefore, the tension of the cable can be estimated as twice the vertical reaction force sensed by the load cell ($T \approx 2F_1$).

b) Ankles Module

The ankles module uses a spatial parallel cable-driven solution of four cables to control the force applied at the patient's ankles to assist in following specific cartesian 3D gait trajectories. The force transmission to the ankles is achieved using modified commercial foot straps designed for cable machines and resistance bands (SYL Fitness®) (Fig. 2b). These modified ankle straps were connected to the module using 8xbraided Kevlar® wires of 0.5mm diameter with a tensile strength of 45.4kg (SeaKnight®).

Actuation. To assist the movement of the ankles along their gait trajectories, each ankle is powered by four direct-drive outrunner brushless motors, specifically the DUAL SHAFT MOTOR – D6374 150KV (OdriveRobotics, United States), providing up to 3.89Nm (nominal torque) and 5760rpm (no load), which translates to: 13.9Kg per cable an d cable speeds of 16.9m/s for drum radii of 0.028m.

Sensors. Cable lengths are measured using AMT102-V encoders (CUIDevices, United States), fixed to the cable motors. Meanwhile, ankle positions are estimated through the application of forward kinematics, mirroring the methodology employed for the pelvis. The interaction of ankle forces is derived from the measured motor current profiles, leveraging the fact that the outrunner brushless motors utilized exhibit minimal torque resistance and operate via direct drive.

c) *Traction Module*

The traction module assists translation and rotation of the whole platform according to the patient's estimated motion intention. It is composed of four 254mm diameter aluminium mecanum wheels with bearing shafts at 45º and load capacities of 40kg each (Nexus Robot, China), Fig. 1.

Actuation. To assist patient motion in space, the traction module uses four direct drive brushless EC 90 Flat 600W motors (MAXON, Switzerland), one per mecanum wheel, supporting up to 1.5N/m (nominal torque) and 2080 rpm (no load).

Sensors. To measure the platform orientation, a BNO055 IMU sensor (BoschSensortec, Germany) is mounted on the front portion of the frame. For monitoring wheels positions, velocities, the system integrates AMT102-V encoders (CUIDevices, United States) for each wheel. Torques of the wheels are estimated in a manner akin to the ankle module, through the measured currents from the brushless direct drive motors.

2) System Architecture

The system presents a bio-inspired control architecture designed to mirror the Central Nervous System (CNS) organization (Fig. 3), [23]. This architecture is divided into three hierarchical levels: *1) high level*: representing the "perception-intention / voluntary commands" encompassing a clinical interface designed for adjusting spatiotemporal gait parameters, regulating the level of assistance or body weight support, and monitoring patient kinetics and kinematics; *2) middle level*: representing the "central pattern generator", represented as a gait pattern generator developed by the authors, [24], which coordinates the motion of the D2W modules (pelvic, ankles, and traction) in real-time and customizes the gait trajectories according to the patient's characteristics; *3) low level*: representing the "execution", including the real-time control algorithms which oversee the operation of the modules' actuators and sensors.

The platform's main control parameters (bodyweight support, level of assistance at the ankles, and gait speed) as well as the patient's measured kinematic and kinetic profiles

are controlled and monitored in real-time from the clinician interface at the high level. This interface has been developed as an easy-to-use software to command and monitor D2W through a web interface running local as a server in the robot computer built using HTML, NodeJS, JS, CSS and ROS2.

The D2W module actuations are synchronized in the *middle level* using a gait pattern generator, enabling the system to estimate the patient's three-dimensional joint trajectories and their gait velocity in real-time, [24]. These estimated trajectories are then used as setpoints to synchronize the assistance provided by the low-level modules.

The low-level modules (pelvic, ankles, and traction) are responsible for controlling the patient motions, and are synchronized by the gait generator. The modules' controllers were programmed in C++ and Python and subsequently embedded as ROS2 nodes. Each module communicates with its respective sensors and actuators at high frequencies (>1kHz) and directly control the individual motor positions/currents.

All three-layer nodes run on single board computers (SBC) LattePanda 3 Delta 864 8GB RAM/64GB eMMC (Lattepanda, China), OS Ubuntu 20.04 with a PREEMP_RT patch to archive soft real-time performances, [25]. The communication method used is based on Robot Operating System 2 (ROS2) [26].

III. Modelling and Control

A. Cables-driven systems

While both the pelvic and ankle modules contribute to motion assistance through the management of cable lengths and tensions, they vary in their kinematic setups. The pelvic module adopts a suspended cable-driven approach, featuring four motors positioned at the top of the structure, (Fig. 4, *Top schematic*), whereas the ankle module employs non-suspended configurations, incorporating two frontal and two rear motors on each side, thus creating a trapezoidal workspace, (Fig. 4, *Botton schematic*).

Although both the pelvic and ankles modules assist motion by controlling cable lengths/tensions, they differ in kinematic configurations. The pelvic module uses a suspended cable-driven approach with four motors placed at the top of the structure, (Fig. 4, *Top schematic*) while the ankles module uses non-suspended configurations with two frontal and two rear motors for each side, generating a trapezoidal workspace,

Both systems however calculate the three-dimensional joint trajectory setpoints and body weight support force vectors by mapping these into the cable-space as cable lengths through inverse kinematics or cables tensions through a kinetic formulation.

1) Inverse Kinematics

The inverse kinematics approach ($\boldsymbol{\varphi}^{\mathrm{IK}}$) to obtain the cable lengths $\bar{l} = [\bar{l}_1 \dots \bar{l}_m]$ of a cable driven system is defined as:

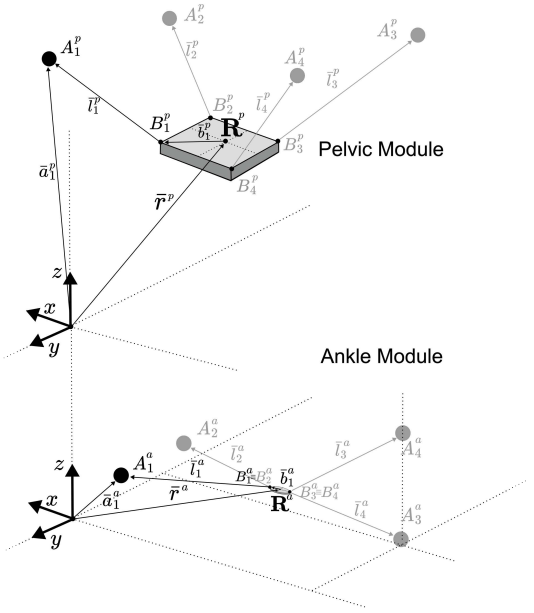

Fig. 4. Geometric schematic of the pelvic and ankles modules; where are represented the joint's j - i^{th} cable vector l_i^j, cable attachment point to the frame A_i^j and corresponding vector $\bar{a}_i^j$, the end-effector cable attachment points and vectors B_i^j and $\bar{b}_i^j$ and the cartesian position vector and rotation matrix of the end-effector $\bar{r}^j$ and , $\boldsymbol{R^j}$. *Top schematic*: the pelvic module presents a suspended kinematic configuration with four motors placed in a rectangular configuration at the top of the structure. *Bottom schematic*: representing the left ankle module, made up of four motors, two frontal motors which share "x-z" positions and two rear motors sharing "x-y" positions, to create a 3D workspace.

$$\boldsymbol{\varphi}^{IK}(\bar{r}, \boldsymbol{R}) = \bar{l} \tag{4}$$

$$\bar{r} = \begin{bmatrix} q_x & q_y & q_z \end{bmatrix}' \tag{5}$$

$$\boldsymbol{R} = \boldsymbol{R}_{q_{roll}} \boldsymbol{R}_{q_{pitch}} \boldsymbol{R}_{q_{yaw}} \tag{6}$$

$$\bar{l}_i = \bar{a}_i - \bar{r} - \boldsymbol{R}\bar{b}_i \qquad for \;\; i = 1, \dots, m \tag{7}$$

$$\bar{u}_i = \frac{\bar{l}_i}{||\bar{l}_i||}, \tag{8}$$

where $\bar{r}$ ($\bar{r} \in \mathbb{R}^3$) represents the end-effector's cartesian position with respect to the platform's frame origin of coordinates, R ($R \in \mathbb{R}^{3x3}$) is the end-effector rotation matrix; $\bar{l}_i$ is the i^{th} cable vector; $\bar{a}_i$ ($\bar{a}_i \in \mathbb{R}^3$) defines the cartesian position of the i^{th} pulley with respect to the origin of coordinates; $\bar{b}_i$ ($\bar{b}_i \in \mathbb{R}^3$) is the cartesian positions of the i^{th} cable's anchor point to the end-effector with respect to the end-effector's reference system, m is the number of cables and $\bar{u}_i$ is a unit vector pointing from the end-effector to the structure.

2) Forward Kinematics

The system modules do not directly measure the end-effector pose however this can be computed through forward kinematics ($\boldsymbol{\varphi}^{\mathrm{DK}}$).

In contrast with the $\boldsymbol{\varphi}^{\mathrm{IK}}$ computation, solving the forward kinematics problem in a cable-driven system is a more complicated task. Depending on the cable lengths, $\bar{l}$, and the robot configuration, an infinite number of solutions are

possible given the mathematical definition of poses involve the intersection between i spheres of radius $||\bar{l}_i||$ with origins in $\bar{a}_i$, [27]. This problem it is commonly solved by applied numerical approaches [22], such as nonlinear least squares data fitting such as:

$$\psi_i(\bar{l}_i, \bar{r}, \boldsymbol{R}) = ||\bar{a}_i - \bar{r} - \boldsymbol{R}\bar{b}_i||^2 - ||\bar{l}_i||^2 = 0 \qquad (9)$$

$$\Phi(\bar{l}) = min \sum_{i=0}^{N-1} \psi_i \,, \qquad (10)$$

where ψ_i is the i^{th} cable's length error function used to minimize the function Φ, that represent the sum of all the errors ψ_i.

Combining these equations for the pelvic module, a system with six degrees of freedom (6DoF) and four cables, results in an indeterminate system characterized by six unknown variables and four cable equations. To reduce the number of unknowns and create a determinate problem, the system was simplified by incorporating pelvic orientation information (3 rotations from the IMU that define the rotational matrix **R**).

For the ankle orthosis system, which also employs a four-cable, 6-DoF setup, a similar dimensional reduction is not feasible due to the absence of rotational data. Attaching IMUs directly to the feet was avoided to reduce the complexity and bulk of wiring needed, which could hinder patient comfort and mobility. As a result, the ankle positions and orientations are estimated using nonlinear least squares data fitting based on (9) and (10).

3) Statics

Assisting gait requires that forces be applied to the patients. To map the cable tensional force modules, T_i, to end-effector wrench, $\bar{f}$, the following static equations are applied:

$$\sum_{i=1}^{m} \mathrm{T}_i \bar{u}_i + \bar{\mathrm{F}} = 0 \qquad (11)$$

$$\sum_{i=1}^{m} \bar{b}_i \times \mathrm{T}_i \bar{u}_i + \bar{\tau} = 0 \qquad (12)$$

$$\underbrace{\begin{bmatrix} \bar{u}_1 & \cdots & \bar{u}_m \\ \bar{u}_1 \times \bar{u}_1 & \cdots & \bar{u}_m \times \bar{u}_m \end{bmatrix}}_{\boldsymbol{A}^T(\bar{r}, \boldsymbol{R})} \underbrace{\begin{bmatrix} T_1 \\ \cdots \\ T_m \end{bmatrix}}_{\bar{\mathrm{T}}} = \underbrace{\begin{bmatrix} \bar{F} \\ \cdots \\ \bar{\tau} \end{bmatrix}}_{\bar{f}} \qquad (13)$$

where $\boldsymbol{A}^T$ is called the structure matrix and represents the transpose of the Jacobian matrix [27], $\bar{\mathrm{T}}$ is the vector of cable tensions modules and $\bar{\mathrm{F}}$ and $\bar{\tau}$ are the cartesian force and torque applied at the end-effector that define the wrench $\bar{f}$.

B. Pelvic Control

The pelvic module plays a dual role in the rehabilitation system: tracking the three-dimensional gait trajectories output by the gait generator, $\phi^*(\bar{r}(t), \boldsymbol{R}(t))$, and actively managing the desired bodyweight support expressed as the target vertical force $\bar{\mathrm{F}}_z(t)^*$, (Fig. 5). The implemented bodyweight controller compensates for errors in vertical force using a force-position PID approach. This force error, $\xi_{\bar{\mathrm{F}}_z}(t)$, is obtained by subtracting the sensed wrench, $\bar{f}(t)$, from the target support force vector $\bar{\mathrm{F}}_z(t)^*$, where $\bar{f}(t)$ is obtained by constructing the $\boldsymbol{A}^T$ matrix based on the computed pelvis

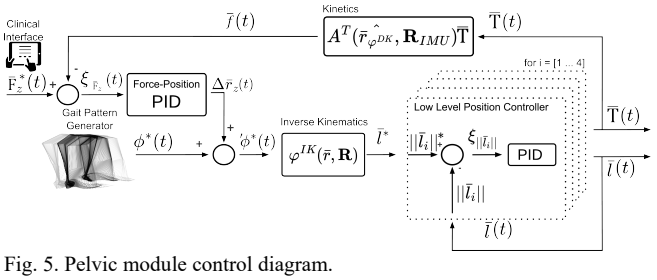

Fig. 5. Pelvic module control diagram.

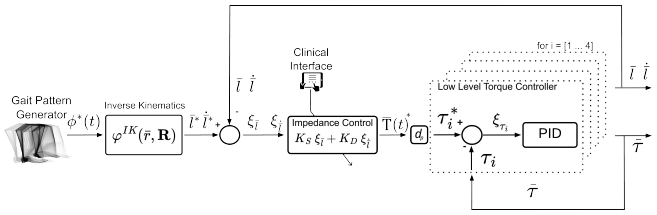

Fig. 6. Ankles control diagram.

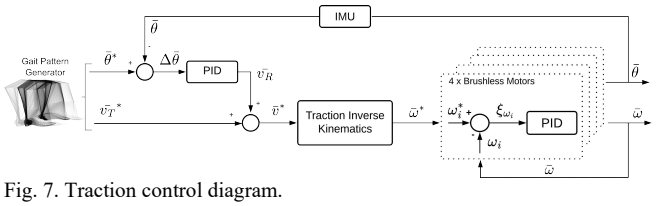

Fig. 7. Traction control diagram.

position, $\widehat{\bar{r}_{\boldsymbol{\varphi}^{DK}}}$, from the forward kinematics, and the sensed cables tensions, $\bar{\mathrm{T}}$ and applying (13) as:

$$\bar{f} = \boldsymbol{A}^T\left(\widehat{\bar{r}_{\boldsymbol{\varphi}^{DK}}}, \boldsymbol{R}_{IMU}\right)\bar{T} \qquad (144)$$

The force-position controller's output represents the vertical position increments, $\Delta\bar{r}_z$, of the end-effector target position which can be used to adjust the supported vertical load. This increment, $\Delta\bar{r}_z$, is added to the gait generator trajectory setpoints to yield an adapted setpoint, $'\phi^*$ which is then mapped to the cable-space using inverse kinematics ($\boldsymbol{\varphi}^{\mathrm{IK}}(\phi^*)$). The resultant cable lengths are controlled by the low-level Dynamixel position PID.

C. Ankles Control

To ensure that patients' lower limbs followed natural gait trajectories during rehabilitation, an Assist-As-Needed (AAN) control strategy was implemented at the ankles module. This strategy smoothly tracks the joint trajectories, ϕ^*, provided by the gait generator, using an impedance-based controller for each cable actuator, (Fig. 6).

The implemented controller initially maps the ankles trajectories during gait into the cable-space using inverse kinematics, $\boldsymbol{\varphi}^{\mathrm{IK}}(\phi^*)$**.** Based on the computed cables' lengths and velocities it is applied the general mechanical impedance model, F = ($K_S\,\xi_{\bar{l}} + D\,\xi_{\dot{\bar{l}}}$), [28], such that the cables perform as spring-damping actuators. The position and velocity errors of the cables, $\xi_{\bar{l}}\ \xi_{\dot{\bar{l}}}$, are mapped to tension forces, $\bar{\mathrm{T}}$. These forces are then converted to torque control inputs, τ_i, by multiplying by the pulley radius, d_p. Finally, the resulting torque inputs are controlled by the low-level PID torque

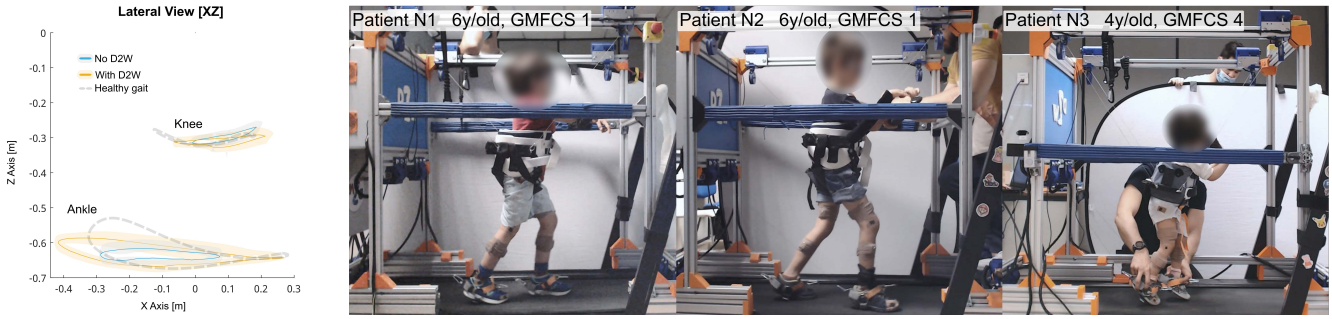

Fig. 8. Lateral view of the three patients engaged in this Discover2Walk preliminary evaluation and a comparison of the average sagittal trajectories of patient N1 during their last therapy session (leftmost figure). Three gait profiles are shown: the blue traces illustrate the patients' natural gait patterns without the system, the orange traces illustrate the altered gait profiles when aided by the platform, and the grey dotted traces illustrate the healthy mean gait trajectory given by the gait generator.

controllers embedded on the Odrive drivers. The "level of assistance" felt by the patient is determined by the stiffness, K, and damping, D, coefficients of the impedance model. To provide the clinicians with an easy-to-use selection method and avoid unstable configurations a lookup table was created with ten pre-tuned impedances with stiffness values raging form 0 to 300 and dumping from 0 to 20.

D. Traction Control

To assist the user's motion around the environment, an omnidirectional traction module was built to support the platform. The system consists of four mecanum wheels distributed with two in the front and two in the rear. The inverse kinematics of the module, assuming no wheel sliding, are defined by:

$$\begin{bmatrix}\omega_1\\ \omega_2\\ \omega_3\\ \omega_4\end{bmatrix} = \frac{1}{r}\begin{bmatrix}1 & -1 & -(a+b)\\ 1 & 1 & -(a+b)\\ 1 & -1 & (a+b)\\ 1 & 1 & (a+b)\end{bmatrix}\begin{bmatrix}v_x\\ v_y\\ \omega\end{bmatrix}, \qquad (15)$$

where, w_i is the angular velocity of the wheels in [rad/s], r is the wheel radius in meters [m], a and b are the distances between the wheel and the centre of the robot in x and y, respectively, and v_x and v_x are the planar linear velocity components and ω the angular velocity of the system, [29].

The traction control loop also requires two inputs: 1) the desired orientation $\bar{\theta}^*$ and 2) the selected linear velocity $\bar{v}_T^*$. The orientation of the platform is controlled based on the correction readings of the IMU attached to the platform frame. The output of this controller, $\bar{v}_R^*$, is added to the linear velocity as an angular velocity component to yield the final target velocity vector $\bar{v}^*$. From $\bar{v}^*$ the wheel velocities, $\bar{\omega}^*$, are obtained usign the aforementioned inverse kinematics and controlled at the low-level using the PID velocity controller embeded in Odrive motor drivers, (Fig. 7).

IV. Preliminary Evaluation of Discover2Walk

The technical evaluation of the Discover2Walk system was conducted with a focus on the functional capabilities of the system. We evaluated the innovative combination of cable-driven pelvis assistance, bodyweight support, and ankle assistance. As a result, the omnidirectional platform was substituted with a treadmill to eliminate the potential complexities introduced by the omnidirectional motion of the traction system, (Fig. 8).

We validated the device with a small group of subjects comprising two six-year-old boys (N1 and N2) of 115cm - 20Kg and 121cm - 23Kg respectively. Both boys were diagnosed with Cerebral Palsy (CP), classified as Gross Motor Function Classification System (GMFCS) Level 1, with asymmetric spastic diplegia, more severe on the right side Additionally, the group included a four-year-old girl of 94cm – 12Kg and GMFCS level 4. The intervention protocol for the two boys was executed over 4-6 weeks, entailing 10 sessions, each lasting up to one hour, per patient in the Hospital Niño Jesus de Madrid (HNJ). Initial sessions were dedicated to familiarization with the D2W modules, while subsequent sessions focused on active gait training, with the intent of gradually reducing assistance levels (both in ankles assistance and bodyweight support) while increasing gait speed. This approach aimed to challenge the participants and evaluate their adaptability and the effectiveness of the D2W platform. For the four-year-old girl classified as GMFCS level 4, the protocol was adapted due to her pronounced motion limitations and spasticity. These sessions served as a proof-of-concept, exploring the system's capability to offer therapeutic benefits and expose her to rehabilitation activities, highlighting the system's adaptability to varied pediatric neuro-motor challenges.

For a comprehensive analysis, the change in various system metrics, including: 1) the position error and assistance torque of the ankles modules; 2) the amount of weight support provided; and 3) the treadmill walking speed, were tracked across sessions. These measures helped evaluate the robot's effectiveness in assisting these movements and the patients' ability to follow the prescribed gait trajectories.

To better understand the dynamic between patients and robotic assistance, we introduce a novel metric named 'effort', (ϵ). This metric, denoted as the product of the controlled ankle's cable's tensions $\bar{T}$ and ankle's cable length position errors $\xi_{\bar{l}}$, serves as a quantitative indicator of the robot's engagement in guiding patient's legs through prescribed gait trajectories, thereby directly correlating module error and assistance. The rationale behind this metric draws from the fundamental principle of work, expressed as $W = Fd$, where W denotes work, F signifies force, applied over a distance, d.

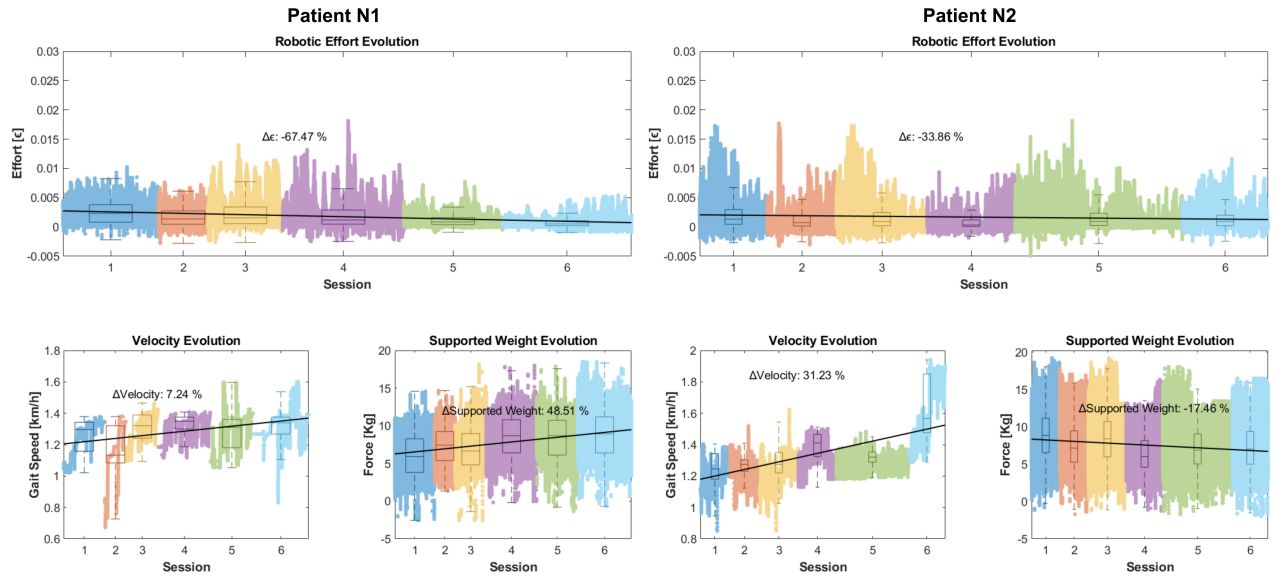

Fig. 9. Comparative analysis of key rehabilitation metrics across therapy sessions for two pediatric patients. The figures on the left represent Patient N1, exhibiting a consistent decrease in robotic effort (Δ : -67.47%), increase in gait speed (Δ : 7.24%), and a rise in weight support (Δ : 48.51%). The figures on the right pertain to Patient N2, showing a marked decrease in robotic effort (Δ : -33.86%), an increase in gait speed (Δ : 31.23%) , and a reduction in weight support (Δ : -17.46%) .

In our specific context, F is represented by $\bar{T}$ (which indicates the level of assistance rendered by the robot), while d can be understood as the position error $\xi_{\bar{l}}$ (depicting the extent of deviation from the ideal trajectory in the patient's movement). To analyse changes in ϵ, walking speed, and body weight support across the therapeutic sessions, we conducted a linear regression analysis using Matlab2022®. This comprehensive approach enables us to discern patterns and quantify the impact of these variables on the therapeutic process.

The analysis revealed encouraging trends for both male participants, (Fig. 9). Patient N1 exhibited a progressive and consistent decrease in the robotic effort of -67.47% relative to the initial session (-64.88% for the left leg and -69.03% for the right leg), indicating symmetrical improvement and equal limb engagement in the rehabilitation sessions. Despite an increase in the applied weight support of 48.51% relative to the first session, gait speed was observed to increase across sessions (7.24 %), suggesting a shift towards more confident and faster walking patterns. Patient N2's data also revealed a decrease in robotic effort of -33.86 % (-31.35 % for the right leg and -38.2% for the left leg). This improvement was accompanied by an increase in gait speed (31.23%) and a decrease in weight support (-17.46%) indicating enhanced motor control and a growing ability to support their own weight.

These outcomes, marked by reduced reliance on robotic assistance and improved gait speed, underscore the Discover2Walk system's potential in advancing pediatric rehabilitation towards greater independence and motor function recovery.

V. Conclusion

This work presents the Discover2Walk (D2W), a novel gait rehabilitation platform designed for pediatric early gait rehabilitation. By employing cable-driven soft modules, the D2W platform addresses several limitations inherent in traditional rigid robotic platforms, such as joint misalignments and restricted degrees of freedom. This design allows for potentially more adaptable therapeutic approaches that can accommodate a variety of body shapes and sizes.

The system was evaluated on three pediatric patients across 10 sessions, including two six-year-olds (GMFCS Level I) and one four-year-old (GMFCS Level IV). This preliminary evaluation aimed to assess the feasibility of the cable-driven actuated modules in supporting pediatric gait rehabilitation. The results showed a trend of decreasing robotic effort required to assist the patients' limbs and an increase in walking speed over the sessions, suggesting potential benefits of the Discover2Walk system for early gait rehabilitation.

However, the current study is limited by the small sample size and the relatively homogeneous characteristics of the participants. To better understand the flexibility and adaptability of the platform across different body types and clinical presentations, further studies involving a broader range of participants and more varied clinical profiles are needed.

Acknowledgement

This work was carried out within the framework of the Discover2Walk project “Development of a robotic platform to help children with Cerebral Palsy discover how to walk”, reference PID2019-105110RB-C31, and the STRIDE project “VALIDACION TECNICA Y ECONOMICA DE LA PLATAFORMA ROBOTICA DISCOVER2WALK PARA EL ENTORNO CLINICO”, reference PDC2022-133898-C31, funded by the Spanish Ministry of Science and Innovation.

REFERENCES

[1] R. Gassert and V. Dietz, "Rehabilitation robots for the treatment of sensorimotor deficits: a neurophysiological perspective," Journal of NeuroEngineering and Rehabilitation 2018 15:1, vol. 15, no. 1, pp. 1–15, Jun. 2018, doi: 10.1186/S12984-018-0383-X.

[2] S. Jezernik, G. Colombo, T. Keller, H. Frueh, and M. Morari, "Robotic Orthosis Lokomat: A Rehabilitation and Research Tool," Neuromodulation: Technology at the Neural Interface, vol. 6, no. 2, pp. 108–115, Apr. 2003, doi: 10.1046/j.1525-1403.2003.03017.x.

[3] J. F. Veneman, R. Kruidhof, E. E. G. Hekman, R. Ekkelenkamp, E. H. F. Van Asseldonk, and H. Van Der Kooij, "Design and evaluation of the LOPES exoskeleton robot for interactive gait rehabilitation," IEEE Transactions on Neural Systems and Rehabilitation Engineering, vol. 15, no. 3, pp. 379–386, Sep. 2007, doi: 10.1109/TNSRE.2007.903919.

[4] C. Bayón et al., "Development and evaluation of a novel robotic platform for gait rehabilitation in patients with Cerebral Palsy: CPWalker," Rob Auton Syst, vol. 91, pp. 101–114, May 2017, doi: 10.1016/j.robot.2016.12.015.

[5] C. Bayon, R. Raya, S. L. Lara, O. Ramirez, I. Serrano, and E. Rocon, "Robotic Therapies for Children with Cerebral Palsy: A Systematic Review," Transl Biomed, vol. 7, no. 1, pp. 1–10, 2016, doi: 10.21767/2172-0479.100044.

[6] J. Kang, D. Martelli, V. Vashista, I. Martinez-Hernandez, H. Kim, and S. K. Agrawal, "Robot-driven downward pelvic pull to improve crouch gait in children with cerebral palsy," Sci Robot, vol. 2, no. July, pp. 1–12, 2017, doi: 10.1126/scirobotics.aan2634.

[7] C. Bayón et al., "A robot-based gait training therapy for pediatric population with cerebral palsy: goal setting, proposal and preliminary clinical implementation," J Neuroeng Rehabil, vol. 15, no. 1, p. 69, Dec. 2018, doi: 10.1186/s12984-018-0412-9.

[8] S. Cho, K. Do Lee, and H. S. Park, "A Mobile Cable-Tensioning Platform to Improve Crouch Gait in Children With Cerebral Palsy," IEEE Transactions on Neural Systems and Rehabilitation Engineering, vol. 30, pp. 1092–1102, 2022, doi: 10.1109/TNSRE.2022.3167472.

[9] X. Chen, C. Ragonesi, J. C. Galloway, and S. K. Agrawal, "Training toddlers seated on mobile robots to drive indoors amidst obstacles," IEEE Transactions on Neural Systems and Rehabilitation Engineering, vol. 19, no. 3, pp. 271–279, 2011, doi: 10.1109/TNSRE.2011.2114370.

[10] D. P. Miller, A. H. Fagg, L. Ding, T. H. A. Kolobe, and M. A. Ghazi, "Robotic Crawling Assistance for Infants with Cerebral Palsy," Artificial Intelligence Applied to Assistive Technologies and Smart Environments: Papers from the 2015 Association for the Advancement of Artificial Intelligence Workshop, pp. 36–38, 2015.

[11] L. A. Prosser, L. B. Ohlrich, L. A. Curatalo, K. E. Alter, and D. L. Damiano, "Feasibility and preliminary effectiveness of a novel mobility training intervention in infants and toddlers with cerebral palsy," Dev Neurorehabil, vol. 15, no. 4, pp. 259–266, Aug. 2012, doi: 10.3109/17518423.2012.687782.

[12] J. H. Martin, S. Chakrabarty, and K. M. Friel, "Harnessing activity-dependent plasticity to repair the damaged corticospinal tract in an animal model of cerebral palsy.," Dev Med Child Neurol, vol. 53 Suppl 4, no. 18, pp. 9–13, Sep. 2011, doi: 10.1111/j.1469-8749.2011.04055.x.

[13] I. Novak et al., "A systematic review of interventions for children with cerebral palsy: state of the evidence.," Dev Med Child Neurol, vol. 55, no. 10, pp. 885–910, Oct. 2013, doi: 10.1111/dmcn.12246.

[14] M. H. McEwan, R. E. Dihoff, and G. M. Brosvic, "Early infant crawling experience is reflected in later motor skill development.," Percept Mot Skills, vol. 72, no. 1, pp. 75–9, 1991, doi: 10.2466/pms.1991.72.1.75.

[15] W. Deng, I. Papavasileiou, Z. Qiao, W. Zhang, K. Y. Lam, and S. Han, "Advances in Automation Technologies for Lower Extremity Neurorehabilitation: A Review and Future Challenges," IEEE Rev Biomed Eng, vol. 11, pp. 289–305, May 2018, doi: 10.1109/RBME.2018.2830805.

[16] C. Siviy et al., "Opportunities and challenges in the development of exoskeletons for locomotor assistance," Nat Biomed Eng, vol. 7, no. 4, pp. 456–472, Apr. 2023, doi: 10.1038/S41551-022-00984-1.

[17] R. C. Browning, J. R. Modica, R. Kram, and A. Goswami, "The effects of adding mass to the legs on the energetics and biomechanics of walking," Med Sci Sports Exerc, vol. 39, no. 3, pp. 515–525, Mar. 2007, doi: 10.1249/MSS.0B013E31802B3562.

[18] A. Schiele and F. C. T. Van Der Helm, "Kinematic design to improve ergonomics in human machine interaction," IEEE Trans Neural Syst Rehabil Eng, vol. 14, no. 4, pp. 456–469, Dec. 2006, doi: 10.1109/TNSRE.2006.881565.

[19] M. Bannwart, M. Bolliger, P. Lutz, M. Gantner, and G. Rauter, "Systematic analysis of transparency in the gait rehabilitation device the FLOAT," 2016 14th International Conference on Control, Automation, Robotics and Vision, ICARCV 2016, 2016, doi: 10.1109/ICARCV.2016.7838710.

[20] V. Vashista, M. Khan, and S. K. Agrawal, "A Novel Approach to Apply Gait Synchronized External Forces on the Pelvis using A-TPAD to Reduce Walking Effort," IEEE Robot Autom Lett, vol. 1, no. 2, p. 1118, Jul. 2016, doi: 10.1109/LRA.2016.2522083.

[21] H. Lamine, M. Amine Laribi, S. Bennour, L. Romdhane, and S. Zeghloul, "Design Study of a Cable-based Gait Training Machine," J Bionic Eng, vol. 14, no. 2, pp. 232–244, Apr. 2017, doi: 10.1016/S1672-6529(16)60394-3/METRICS.

[22] A. Pott, "An Algorithm for Real-Time Forward Kinematics of Cable-Driven Parallel Robots," Advances in Robot Kinematics: Motion in Man and Machine, pp. 529–538, 2010, doi: 10.1007/978-90-481-9262-5_57.

[23] G. Delgado-Oleas, P. Romero-Sorozabal, J. Lora-Millan, A. Gutierrez, and E. Rocon, "Bioinspired Hierarchical Electronic Architecture for Robotic Locomotion Assistance: Application in Exoskeletons," IEEE Access, vol. 11, pp. 131610–131622, 2023, doi: 10.1109/ACCESS.2023.3336003.

[24] P. Romero Sorozabal, G. Delgado-Oleas, A. Gutierrez, and E. Rocon, "Individualized Three-Dimensional Gait Pattern Generator for Lower Limbs Rehabilitation Robots," in IEEE International Conference on Rehabilitation Robotics (ICORR) , Singapore, 2023.

[25] F. Reghenzani, G. Massari, and W. Fornaciari, "The Real-Time Linux Kernel," ACM Computing Surveys (CSUR), vol. 52, no. 1, Feb. 2019, doi: 10.1145/3297714.

[26] D. Casini, T. Blaß, I. Lütkebohle, and B. B. Brandenburg, "Response-time analysis of ROS 2 processing chains under reservation-based scheduling," Leibniz International Proceedings in Informatics, LIPIcs, vol. 133, Jul. 2019, doi: 10.4230/LIPICS.ECRTS.2019.6/-/STATS.

[27] A. Pott, Cable-driven parallel robots: Theory and application, vol. 120. 2018. doi: 10.1007/978-3-319-76138-1.

[28] N. Hogan, "Impedance Control: An Approach to Manipulation: Part I—Theory," J Dyn Syst Meas Control, vol. 107, no. 1, pp. 1–7, Mar. 1985, doi: 10.1115/1.3140702.

[29] J. Ji, W. Chen, W. Wang, and J. Xi, "Design and control of an omni-directional robotic walker based on human-machine interaction," IEEE Access, vol. 9, pp. 111358–111367, 2021, doi: 10.1109/ACCESS.2021.3103202.